LAWRENCE
LIVERMORE
NATIONAL
LABORATORY

# A SQUID-based microwave cavity search for dark-matter axions

S. J. Asztalos, G. Carosi, C. Hagmann, D. Kinion, K. van Bibber, M. Hotz, L. Rosenberg, G. Rybka, J. Hoskins, J. Hwang, P. Sikivie, D. B. Tanner, R. Bradley, J. Clarke

October 23, 2009

**Disclaimer**

This document was prepared as an account of work sponsored by an agency of the United States government. Neither the United States government nor Lawrence Livermore National Security, LLC, nor any of their employees makes any warranty, expressed or implied, or assumes any legal liability or responsibility for the accuracy, completeness, or usefulness of any information, apparatus, product, or process disclosed, or represents that its use would not infringe privately owned rights. Reference herein to any specific commercial product, process, or service by trade name, trademark, manufacturer, or otherwise does not necessarily constitute or imply its endorsement, recommendation, or favoring by the United States government or Lawrence Livermore National Security, LLC. The views and opinions of authors expressed herein do not necessarily state or reflect those of the United States government or Lawrence Livermore National Security, LLC, and shall not be used for advertising or product endorsement purposes.

# A SQUID-based microwave cavity search for dark-matter axions

S.J. Asztalos*, G. Carosi, C. Hagmann, D. Kinion and K. van Bibber

*Lawrence Livermore National Laboratory, Livermore, California, 94550*

M. Hotz, L. Rosenberg and G. Rybka

*University of Washington, Seattle, Washington 98195*

J. Hoskins, J. Hwang†, P. Sikivie and D.B. Tanner

*University of Florida, Gainesville, Florida 32611*

R. Bradley

*National Radio Astronomy Observatory, Charlottesville, Virginia 22903*

J. Clarke

*University of California and Lawrence Berkeley National Laboratory, Berkeley, California 94720*

(Dated: October 21, 2009)

Axions in the $\mu$eV mass range are a plausible cold dark matter candidate and may be detected by their conversion into microwave photons in a resonant cavity immersed in a static magnetic field. The first result from such an axion search using a superconducting first-stage amplifier (SQUID) is reported. The SQUID amplifier, replacing a conventional GaAs field-effect transistor amplifier, successfully reached axion-photon coupling sensitivity in the band set by present axion models and sets the stage for a definitive axion search utilizing near quantum-limited SQUID amplifiers.

PACS numbers: 14.80.Mz, 95.35.+d

The axion is a hypothetical particle that may play a central role in particle physics, astrophysics and cosmology. Axions are pseudoscalars that result from the Peccei-Quinn solution to the strong CP problem [1–3]. Axions or axion-like particles may also be a fundamental feature of string theories [4]. Low mass axions ($m_a = \mu$eV-meV) may have been produced in the early universe in quantities sufficient to account for a large portion of the cold dark matter in galactic halos [5–8]. These dark matter axions have extremely feeble couplings to normal matter and radiation, but may be converted into detectable microwave photons using the inverse Primakoff effect as first outlined by Sikivie [9, 10]. Searches based on this technique are by far the most sensitive for low mass dark-matter axions. A comprehensive dark matter axion review can be found in [11]. In this Letter we describe the first results from an axion search that uses superconducting (SQUID) electronics, which offer a qualitative improvement in the sensitivity of our search.

The Axion Dark Matter eXperiment (ADMX) has been running in various configurations at Lawrence Livermore National Laboratory (LLNL) since 1996. The ADMX experimental configuration is sketched in Fig. 1. Virtual photons are provided by an 7.6 Tesla magnetic field generated by a large superconducting solenoid with a 0.5 m diameter bore. A cylindrical copper-plated microwave cavity is embedded in the magnet bore, and dark matter axions passing through the cavity can resonantly convert into real microwave photons with energy $E \approx m_a c^2 + \frac{1}{2} m_a c^2 \beta^2$. With expected velocity dispersions of $\beta \sim 10^{-3}$ for virialized dark matter in our galaxy the spread in energy should be $\sim 10^{-6}$ or $\sim 1.2$ kHz for a 5 $\mu$eV axion. The expected power generated by axion-photon conversions is given by [9, 10],

$$P_a = g_{a\gamma\gamma}^2 V B_0^2 \rho_a C_{lmn} \min(Q_L, Q_a), \tag{1}$$

where $g_{a\gamma\gamma}$ is the coupling strength of the axion to two photons, $V$ is the cavity volume, $B_0$ is the magnetic field, $\rho_a$ is the local axion dark matter density, $Q_L$ is the loaded cavity quality factor (center frequency over bandwidth), $Q_a \sim 10^6$ is the axion signal quality factor (axion energy over energy spread) and $C_{lmn}$ is a form factor for the TM$_{lmn}$ cavity mode (overlap of static B field with oscillating E field of the particular mode). In ADMX the TM$_{010}$ mode provides the largest form factor ($C_{010} \approx 0.69$) [12] and its frequency can be moved up by translating copper-plated axial tuning rods from the edge of the cavity to the center. Given the experimental parameters, $P_a$ is expected to be of order $10^{-22}$ W. The coupling constant $g_{a\gamma\gamma} \equiv g_\gamma \alpha / \pi f_a$, where $\alpha$ is the fine-structure constant, $f_a$ is the "Peccei-Quinn symmetry breaking scale" (an important parameter in axion theory), and $g_\gamma$ is a dimensionless model-dependent coefficient of $O(1)$. A representative choice within the so-called KSVZ models (for Kim-Shifman-Vainshtein-Zakharov) has $g_\gamma \sim 0.97$ [13, 14] while one particular choice within the GUT inspired DFSZ (for Dine-Fischler-Srednicki-

*Currently at XIA LLC, 31057 Genstar Rd., Hayward CA, 94544.
†Currently at Pusan National University, Busan, 609-735, Republic of Korea.
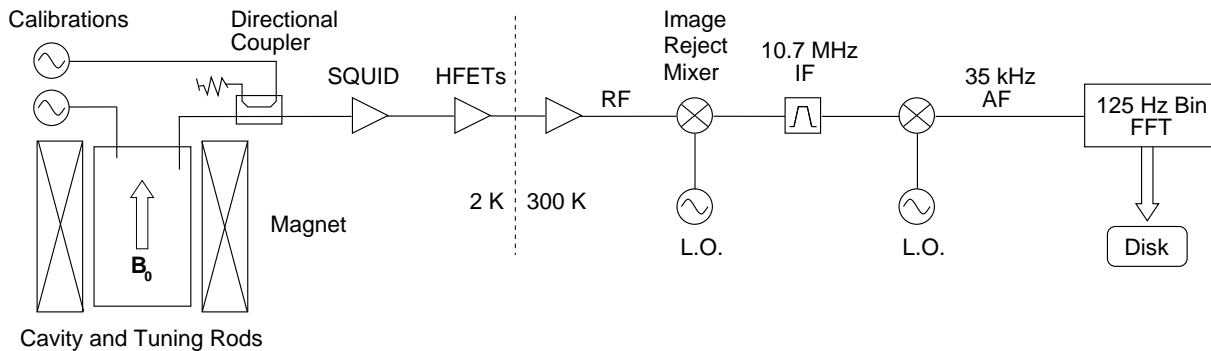
FIG. 1: Schematic of ADMX experiment. The lower left-hand oscillator sweeps in signal to a weakly coupled port to determine the resonant mode of the cavity while the upper left-hand oscillator allows for a reflection check in order to critically couple the signal antenna to the cavity.

Zhitnitshii) family of models has $g_\gamma \sim -0.36$ [15, 16]. Detailed experimental descriptions along with previous results can be found in [17] and [18].

The sensitivity of the detector is set by the Dicke radiometer equation [19] in which the signal-to-noise ratio ($SNR$) is,

$$SNR = \frac{P_a}{P_N}\sqrt{Bt} = \frac{P_a}{k_B T_S}\sqrt{\frac{t}{B}}. \qquad (2)$$

Here $P_N$ is the system noise power, $k_B$ is Boltzmann's constant, $B$ is the bandwidth and $t$ is the integration time. The system noise temperature $T_S$ is the sum of the physical cavity temperature $T_C$ and the amplifier noise temperature $T_A$. In searching the mass range for an axion with a given coupling $g_{a\gamma\gamma}$ the scan rate is given by

$$\frac{dm_a}{dt} \propto (B_0^2 V)^2 \cdot \frac{1}{T_S^2} \qquad (3)$$

while, given a specific logarithmic scan rate, the smallest detectable coupling ($g_{a\gamma\gamma}^2 \propto P_a$) is given by

$$g_{a\gamma\gamma}^2 \propto (B_0^2 V)^{-1} T_S \qquad (4)$$

Clearly there is a high premium on reducing $T_S$ to its lowest achievable value. Earlier experiments used balanced GaAs heterostructure field-effect transistor (HFET) cryogenic amplifiers built by the National Radio Astronomy Observatory (NRAO) [11, 20] for first stage amplification. HFET amplifiers have noise temperatures that drop as their physical temperature is lowered until around 10 to 20 K, at which point the noise temperature plateaus at a value of a few K. Though extremely quiet by radio astronomy standards, in this application their intrinsic noise of a few K severely limited the scan speed and coupling reach of previous experiments. This limitation spurred the development in the late 1990's of replacement amplifiers for ADMX based on dc SQUIDs (Superconducting QUantum Interference Devices). Although dc SQUIDs have been used as amplifiers for decades [21], they suffer from severe gain roll-off at

microwave frequencies due to parasitic coupling between the input coil and SQUID washer. The SQUID amplifiers developed for ADMX are based on a novel geometry [Fig. 2], where the input coil is replaced by a resonant microstrip input coil [22]. The SQUID amplifiers used in the axion search reported here have *in situ* microwave power gain of $\sim 10$ dB in the frequency range scanned.

Unlike HFET amplifiers, SQUID amplifier noise temperature continues to drop with decreasing temperature until it approaches the quantum noise limit ($T_Q = \hbar\omega/k_B \approx 50$ mK at 1 GHz). Fig. 3 shows this behavior for two SQUIDs operating on resonance at 684 and 702 MHz. At the lowest temperatures their noise temperature of $47 \pm 5$ mK are a factor of 1.4 above the quantum-limited noise temperature of 33 mK. Though future experiments will have dilution refrigeration to cool the SQUID and cavity to $\sim 100$ mK, the current phase of the experiment used pumped liquid helium (LHe) to maintain cavity and SQUID temperatures of $\sim 2$ K. For most of the data run, the cavity was kept under vacuum and cooled via a small LHe reservoir fixed to the cavity top and pumped down to $\sim 1$ Torr. The SQUID housing was thermally attached via a copper cold finger and copper strap to this reservoir. Regions in frequency where a TE or TEM mode crossed the $TM_{010}$ mode were scanned by filling the cavity with superfluid LHe which shifted the mode-crossing by $\sim 3\%$.

Given its extraordinary flux sensitivity, placing a SQUID amplifier in the strong fringe field of the ADMX magnet provided an additional challenge. To solve this, the SQUID was placed $\sim 1$ m above the top of the solenoid where the axial field has diminished to $\sim 0.5$ T and inside a superconducting "bucking magnet" solenoid which canceled the fringe field to a few 100 $\mu T$. Two nested layers of cryogenic $\mu$-metal further reduced the field, and the SQUID itself was placed in a superconducting, lead-plated amplifier housing to reject any remaining stray field. Hall sensors inside and outside the $\mu$-metal shielding monitored the magnetic fields.
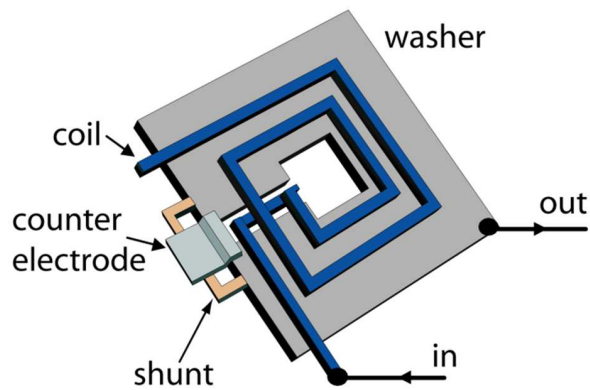
Following the SQUID were second- and third-stage
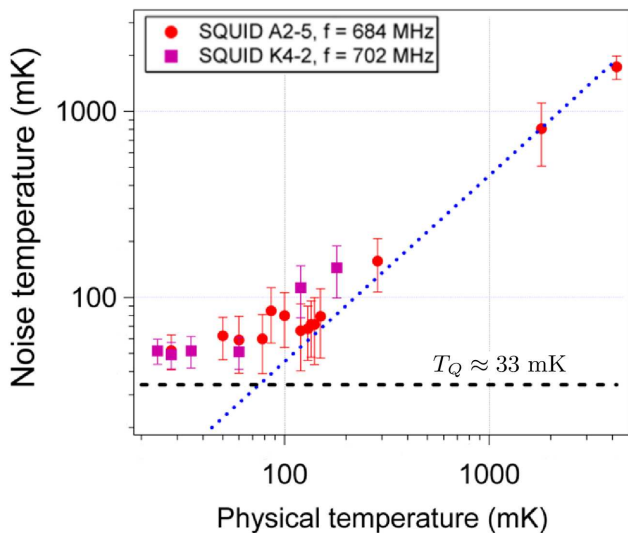
FIG. 2: Schematic of a microstrip SQUID amplifier.



FIG. 3: Noise temperature of two representative SQUID amplifiers (with resonant frequency **f**) as a function of physical temperature. $T_Q$ is the quantum noise temperature at $\approx 700$ MHz.
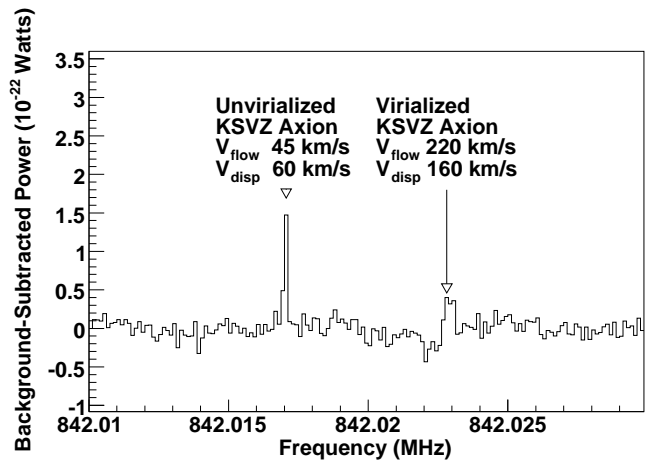


FIG. 4: Dark matter axion signals simulated with Monte Carlo and imposed on real data for two dark matter axion distribution models (masses arbitrarily chosen).

s. This resulted in a 400 point, single-sided 125 Hz resolution power spectrum. After each 80 s acquisition, the tuning rods moved the $TM_{010}$ mode by $\sim 2$ kHz. The loaded $Q_L$ was remeasured before another 80 s acquisition began at the new frequency. The overlap between adjacent spectra was such that each 125 Hz frequency bin had $\sim 25$ minutes of exposure.

A high resolution channel, not used in this analysis, is sensitive to axion spectral lines much narrower than 125 Hz. This channel applies the 35 kHz signal to a 6.5 kHz-wide passband filter, which is then mixed to an AF of 5 kHz. This is digitized and a single power spectrum is obtained by acquiring $2^{20}$ points over 53 s for a Nyquist frequency resolution of 19 mHz. Results from this channel will be described in a future paper.

Each raw power spectrum was corrected for the receiver input-to-output transfer function. The frequency response of the transfer function is dominated by the IF crystal filter, and its effect was determined by an average of many spectra taken over a range of cavity frequency settings. The remaining frequency variation of the transfer function, primarily due to frequency dependent interactions of the cavity, transmission line and amplifier input, was removed by fitting and dividing each spectra by a 6 parameter polynomial. Spectra for which the chi-square of this fit (excluding peaks) was greater than 1.5 were discarded as the receiver transfer function may have been poorly estimated in those cases.

Frequencies were rescanned and the power in the bins averaged until the expected signal-to-noise for a KSVZ axion at a dark matter density of 0.45 GeV/cm$^3$ was greater than 3.5. The average signal-to-noise for this run was 10.4. After this, bins of width 125 Hz were examined for excess power above the thermal power level. Bins that had too much measured power to exclude KSVZ axions were rescanned several times, and these spectra averaged with the previous data run. A characteristic of a true
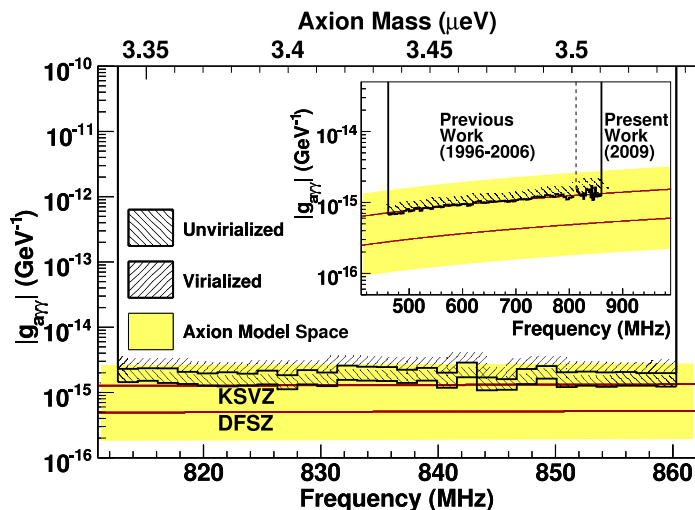
cryogenic HFET amplifiers. They provided an additional 12 dB combined power gain, and contributed a negligible amount to the system noise temperature. The signal was routed via RG-402 coaxial cable to a room-temperature post-amplifier before being coupled to a double-heterodyne receiver, consisting of an image-rejection mixer with an intermediate frequency (IF) of 10.7 MHz. This IF stage included an eight-pole crystal filter with a 30 kHz bandwidth. The signal was then mixed-down a second time with a doubly-balanced mixer to an audio frequency (AF) of 35 kHz. This signal was digitized and analyzed in hardware via fast-Fourier transform (FFT), optimized to search for the fully virialized axion signal. This is our medium resolution channel. At each tuning-rod setting, 10,000 8-msec spectra at 125 Hz Nyquist resolution were added for a total exposure of 80

FIG. 5: Axion-photon coupling excluded at the 90% confidence level assuming a local dark matter density of 0.45 GeV/cm$^3$ for two dark matter distribution models. The shaded region corresponds to the range of the axion photon coupling models discussed in [23].

to set a limit on the product of axion coupling and local dark matter density. Two models for the axion spectral line shape were examined: completely virialized axions with a velocity dispersion of 160 km/s and a velocity relative to earth of 220 km/s, and axions with a velocity dispersion and relative velocity of 60 km/s or less, as would be predicted by a caustic model [25] or a dark disk model [26]. Expected signals for both models superimposed on real data are shown in Fig. 4. Models with lower velocity dispersions produce narrower peaks in the power spectrum, with a consequently higher SNR. The 90% confidence bound on axion coupling with a local dark matter density of 0.45 GeV/cm$^3$ is shown in Fig. 5.

We exclude at 90% confidence realistic axion models of dark matter, with a local density of 0.45 GeV/cm$^3$ for axion masses ranging 3.3 $\mu$eV to 3.53 $\mu$eV. This extends the excluded region from [18], excluding plausible axion dark matter models from 1.9 $\mu$eV to 3.53 $\mu$eV. Additionally, we have demonstrated the first application of a dc SQUID amplifier in a high field environment with a noise temperature comparable to our previous runs. In the next phase of ADMX, the SQUID and cavity will be cooled with a dilution refrigerator to 100 mK, allowing the detector to scan over the plausible axion mass range several hundred times faster at the present sensitivity, or to be sensitive to even the most pessimistic axion-photon couplings over the entire axion mass range while still scanning ten times as fast as the present detector.

axion signal is that it would reappear in a rescan, whereas statistical fluctuations or transient environmental signals would not. Such rescans were performed within weeks of the original scan, during which a putative axion signal could have shifted at most 20 Hz due to the Earth's orbit and rotation, far smaller than the medium resolution bin width [24]. In this run, the number of rescans agreed with statistical expectations from thermal noise. No signals were found to persist after the second rescan.

The total power and expected axion SNR were used

[1] R. D. Peccei and H. R. Quinn, Phys. Rev. Lett. **38**, 1440 (1977).
[2] S. Weinberg, Phys. Rev. Lett. **40**, 223 (1978).
[3] F. Wilczek, Phys. Rev. Lett. **40**, 279 (1978).
[4] P. Svrček and E. Witten, J. High Energy Phys. **2006**, 051 (2006).
[5] J. Preskill, M. Wise, and F. Wilczek, Phys. Lett. B **120**, 127 (1983).
[6] L. F. Abbott and P. Sikivie, Phys. Lett. B **120**, 133 (1983).
[7] M. Dine and W. Fischler, Phys. Lett. B **120**, 137 (1983).
[8] J. Ipser and P. Sikivie, Phys. Rev. Lett. **50**, 925 (1983).
[9] P. Sikivie, Phys. Rev. Lett. **51**, 1415 (1983).
[10] P. Sikivie, Phys. Rev. D **32**, 2988 (1985).
[11] R. Bradley et al., Rev. Mod. Phys. **75**, 777 (2003).
[12] H. Peng et al., Nucl. Instrum. Methods A **444**, 569 (2000).
[13] J. Kim, Phys. Rev. Lett. **43**, 103 (1979).
[14] M. Shifman, A. Vainshtein, and V. Zakharov, Nucl. Phys. B **166**, 493 (1980).
[15] A. Zhitnitskii, Sov. J. Nucl. Phys. **31**, 260 (1980).

[16] M. Dine, W. Fischler, and M. Srednicki, Phys. Lett. B **104**, 199 (1981).
[17] L. D. Duffy et al., Phys. Rev. D **74**, 012006 (2006).
[18] S. J. Asztalos et al., Phys. Rev. D **69**, 011101 (2004).
[19] R. Dicke, Rev. Sci. Instrum. **17**, 268 (1946).
[20] E. Daw and R. Bradley, J. Appl. Phys. **82**, 1925 (1997).
[21] J. Clarke, A. Lee, M. Mück, and P. Richards, Squid voltmeters and amplifiers, in *The SQUID Handbook Vol. II: Applications of SQUIDs and SQUID systems*, pp. 1–93, 2006.
[22] M. Mück, M.-O. André, J. Clarke, J. Gail, and C. Heiden, Applied Physics Letters **72**, 2885 (1998).
[23] J. E. Kim, Phys. Rev. D **58**, 055006 (1998).
[24] F.-S. Ling, P. Sikivie, and S. Wick, Phys. Rev. D **70**, 123503 (2004).
[25] L. D. Duffy and P. Sikivie, Phys. Rev. D **78**, 063508 (2008).
[26] J. I. Read, G. Lake, O. Agertz, and V. P. Debattista, (2008), arXiv:0803.2714.